New Apparatus & Upgrades

High-Resolution Micro-CT System using 10-Megapixel-CCD X-ray Detector

A micro-CT (computed tomography) system, shown in Fig. 1, was developed using a 10-megapixel CCD camera for 3D biomedical imaging [1]. The detector consists of a beryllium window for X-ray incidence, a fluorescent screen, an optical mirror, high-numerical-aperture lenses and the CCD camera. X-rays are converted into a visible image on the screen with a thickness of 10 μm. The screen and mirror are built in behind the beryllium window. The mirror deflects the luminescent light by 90° to the lens system that focuses the light onto the camera. The X-ray field of view is 24 mm wide × 16 mm high (4024 × 2648 pixels); each pixel measures 6 × 6 μm^2.

A rabbit auricle specimen implanted with a carcinoma was fixed in formalin and sealed in the specimen case in the micro-CT system (Fig. 1) after a barium sulfate solution was injected into blood vessels as a contrast agent. Projection images were recorded from 1800 views during 180-degree rotation. Three-dimensional images of the specimen, shown in Fig. 2 were obtained by tomographic reconstruction, and small blood vessels induced by the tumor were visualized. The avascular area at the center is dead tumor tissue. In contrast, the number of blood vessels increased markedly around the avascular area, where tumor cells were vital and the tumor's growth rate was rapid.

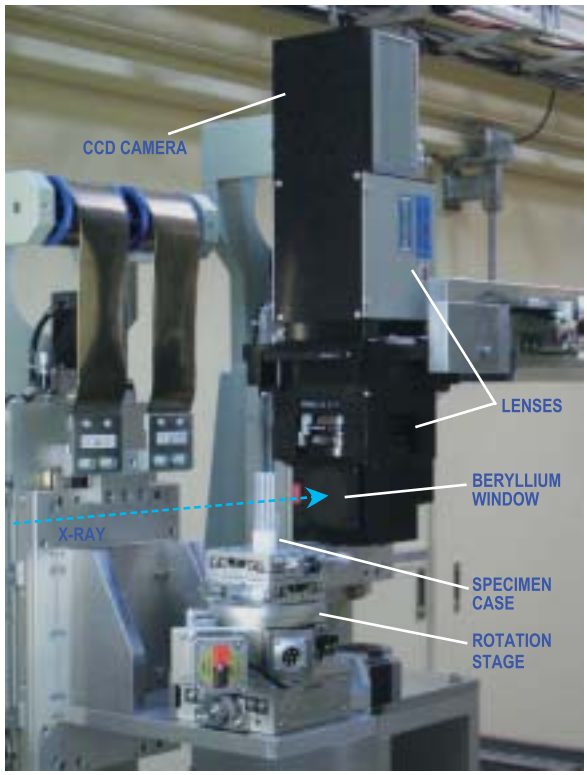

Fig. 1. Micro-CT system with 10 megapixels.

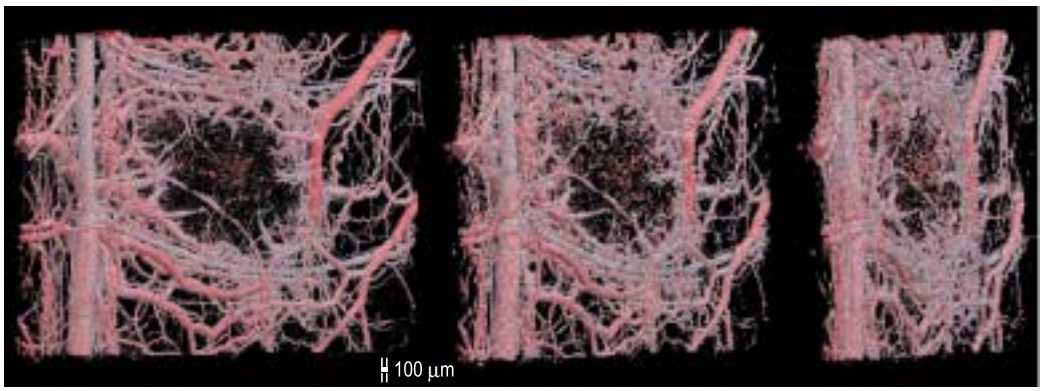

Fig. 2. Three-dimensional images of a tumor surrounded by the network of blood vessels induced by the tumor. The images are shown at viewing angles of 0 (front view), 30, and 60 degrees, from left to right.

Keiji Umetani

SPring-8 / JASRI

E-mail: umetani@spring8.or.jp

References

[1] *K. Umetani, K. Uesugi, N. Yagi, M. Kobatake, A. Yamamoto, T. Yamashita, S. Imai, and Y. Kajihara: to be published in Nucl. Instrum. Meth.*

Extending the Limits of Inelastic X-ray Scattering: 12 Analyzers and 1 meV Resolution

Inelastic X-ray scattering is a technique that pushes the limits of what is possible with even a third generation synchrotron radiation facility: ~meV bandwidths and small inelastic cross sections mean that nearly all experiments are severely flux limited. There is strong impetus to improve the SPring-8 instrument, both to maximize the use of the available flux and to improve the resolution. In fact, better resolution is generally accompanied by a reduction of flux on the sample, and so drives the push to become more efficient. We embarked on an ambitious plan to improve the performance of the **BL35XU** spectrometer [1]: tripling the number of analyzers and improving the resolution to 1 meV. This involved modifying nearly all the optical components of the beamline downstream of the high-heat-load monochromator.

Our first step was reduction of the heat-load onto the backscattering crystal. The ~100 mW monochromatic X-ray beam is enough to cause local heating and lattice distortions at the level of parts in 10^8, degrading the resolution. While this problem was partially solved by using a grazing incidence geometry to distribute the power on the backscattering crystal [2], additional power load reduction was needed to attain 1 meV resolution. In the original beamline design [1], Fig. 1(a), a pair of Si (111) crystals was used *downstream* of the backscattering monochromator to shift the beam vertically and provide space at the sample position. We moved these crystals *upstream* of the backscattering monochromator, Fig. 1(b). The Si(111) crystals used previously were replaced with Si(220) crystals. These crystals, cut asymmetrically, accept the full angular divergence of the beam from the high-heat-load monochromator but reduce the bandwidth of the beam from ~3.5 eV at 25.7 keV after the Si(111) crystals to ~2.1 eV, a crucial reduction in terms of heat load.

The upgrade from 4 to 12 analyzer crystals involved replacing the analyzer stages, slit system and detector on the 10 m arm of the spectrometer, as well as tripling the number of temperature control channels. While no major conceptual changes were needed, a lot of new equipment had to be installed and debugged. The general setup is shown in Fig. 2.

The new crystal mounts and slits were carefully designed to minimize the center-to-center spacing of the analyzers, as this improves the quality of data from both liquids and solids. A 120 mm center-to-center spacing was chosen for the 100-mm-diameter analyzers in the 10-m chamber. Likewise, the slit system required some care, with, finally, a venetian-blind-style system (see Fig. 2) allowing maximum angular acceptance with little dead space.

A new 12-channel detector system was also installed near the sample location with detector elements both above and below the path of the beam from the sample. The detector elements are CZT and operated at room temperature. They perform very well, with good pulse height response (3 to 4 keV FWHM, without a low-energy tail), essentially 100% stopping power, and low dark-count rates, ~ 5×10^{-4} Hz in our energy range of interest, 16-26 keV.

Present spectrometer performance is summarized in Table 1, for one of our better analyzer crystals. It is worth emphasizing that the unique two-dimensional analyzer array of this instrument makes it possible to efficiently measure both longitudinal phonons *and* transverse phonons using, respectively, horizontal and vertical lines of analyzers along high symmetry directions.

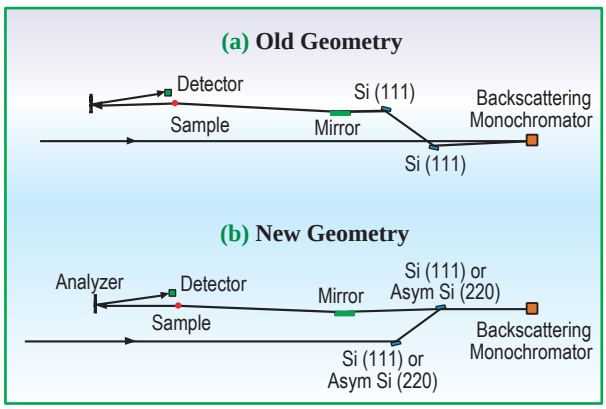

Fig. 1. Re-arrangement of the optics to allow 1 meV energy resolution.

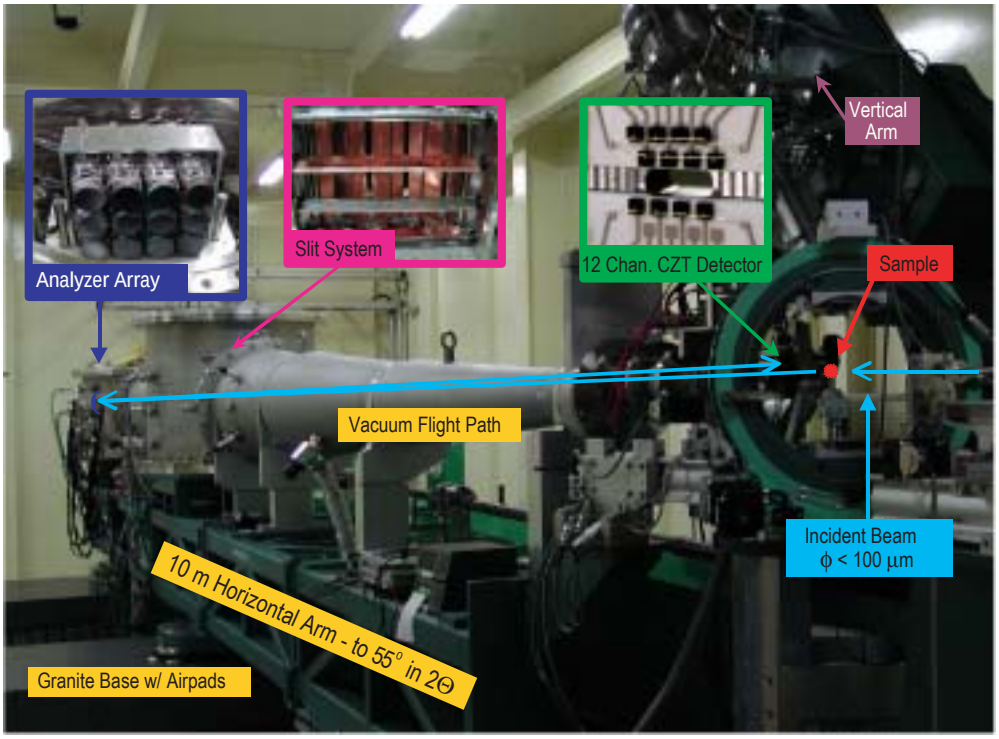

Fig. 2. Photograph of the 10 m arm from a viewpoint just upstream of the sample location. Insets show various pieces of equipment, as labeled. Please note the scale changes: the analyzer array has 12 circular analyzers visible, each 10 cm in diameter, while the detector chips are only 2.5 × 2.5 mm^2.

Table I. Summary of spectrometer performance with one of the better analyzer crystals. Spot size ~70 × 90 μm^2. FWHM at the sample.

Si Order (nnn)	Energy (keV)	Single Reflection Bandwidth (meV)	Flux at Sample (GHz)	Resolution FWHM (meV)
8	15.816	4.1	30	5.9
9	17.794	1.8	10	2.9
11	21.747	0.8	4	1.5
13	25.702	0.35	0.7	0.95

Alfred Q. R. Baron*, John P. Sutter and Satoshi Tsutsui

SPring-8 / JASRI

*E-mail: baron@spring8.or.jp

References

[1] A.Q.R. Baron *et al.*: J. Phys. Chem. Solids **61** (2000) 461.
[2] *A.Q.R. Baron, Y. Tanaka and S. Tsutsui, SPring-8 Research Frontiers 2001/2002, p. 104; A.Q.R. Baron et al.: in preparation.*

New Surface Microscopy – Spectroscopic Photo-emission Electron Microscopy and Low Energy Electron Microscopy (SPELEEM) with Synchrotron Radiation

A new type of surface electron microscope (SPELEEM) that uses synchrotron radiation light (SR-SPELEEM) [1] was installed at SPring-8 and has been offered for public use since this year (2004) [2]. This instrument includes a low energy electron microscope (LEEM) and a photoemission electron microscope (PEEM) with an energy filter. This microscope has recently received much attention in the surface science, nanoscience and nanotechnology because it can produce dynamic images of the surface dynamics at a video rate and a wide variety of technical information. For example, it provides high-resolution (better than 10 nm) LEEM images at surface regions, LEED patterns (surface structure analysis possible at 200-300 nmϕ), high-resolution (better than 10 nm) magnetic domain images of single crystals when using an electron spin source, high-resolution (20-50 nm) X-ray photoelectron spectroscopy (XPS) images, high-resolution (50 nm) X-ray absorption near edge spectroscopy (XANES) images and high-resolution (50-100 nm) magnetic domain images of any material with MCD and MLD. In particular, the high-spatial-resolution (20-50 nmϕ) chemical bonding information at surfaces and the magnetic domain images are almost impossible to obtain with other types of instruments. This SPELEEM is now tentatively installed at the public soft X-ray beamline of **BL27SU**, as shown in Fig. 1. Already, several interesting results have been obtained on the studies of chemical bonding in oxidation of Fe surfaces, Co/Si(111) and In/Si(111) surfaces, and magnetic domains in NiO. This type of instrument was, for the first time, installed at ELETTRA (Trieste, Italy) a few years ago, and three other SR facilities (BESSY II, Germany; SLS, Switzerland and DLS, Great Britain) have installed or started to install the same or a similar type of SPELEEM. The SPELEEM will be installed at beamline **BL17SU** from summer 2005,

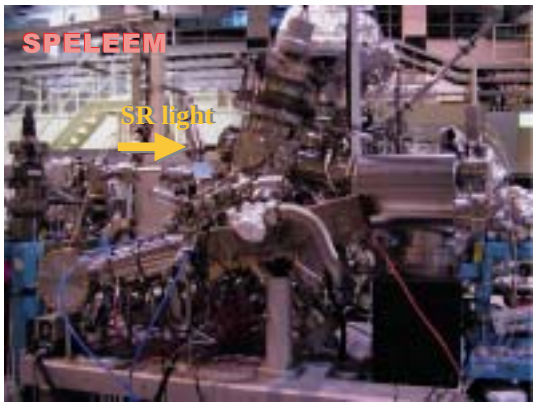

Fig. 1. SPELEEM installed at BL27SU.

which will enable users to address various kinds of issues under much more stable conditions.

Here we describe several examples of results obtained with SPELEEM using BL27SU. Figure 2 shows that "nano-XANES" observation is possible by integrating image intensities in fixed areas of nanosize, while scanning photon energy across target absorption edges. Figure 2(a) shows XANES spectra of a Co-deposited Si(111)7×7 surface [2]. After annealing at *ca.* 600 ºC, the surface exhibited the formation of Co silicide islands, which were surrounded by flat regions, as shown in Fig. 2(b). The red and blue curves in Fig. 2(a) are $L_{2,3}$ XANES

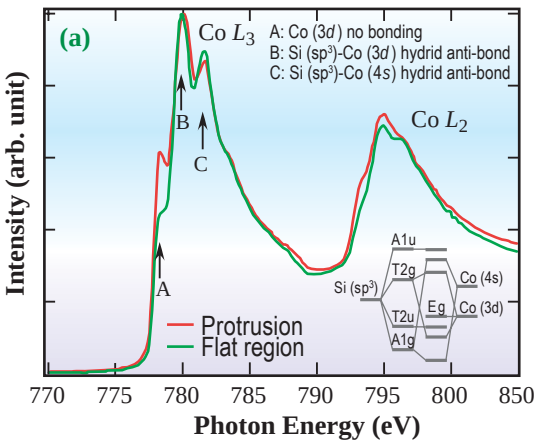

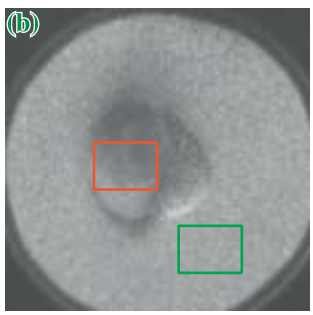

XPEEM (FOV 30 μm, *hν* 780 eV)

Fig. 2. **(a)** Micro-XANES of $CoSi_2$ and the surrounding flat regions. The inset shows the energy diagram of Si-Co hybridization. **(b)** XPEEM image of Co/Si(111) surface. The protrusion corresponds to $CoSi_2$.

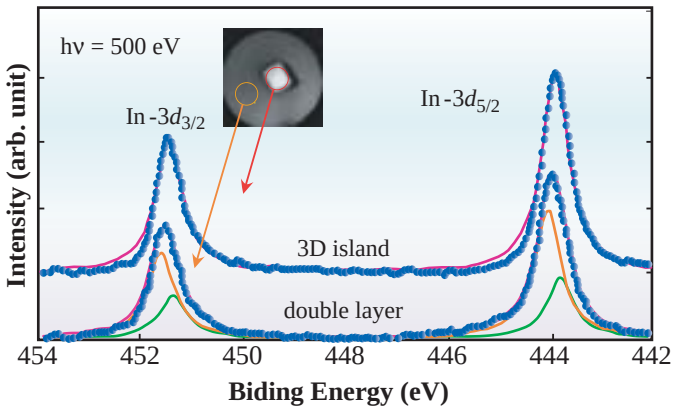

Fig. 3. XPS spectra from double layer and 3D island. Accumulation time for each spectrum was 300 s.

spectra of the island and flat regions, respectively. Three structures are clearly resolved in the L_3 absorption edge. These are assigned to transitions from Co $2p_{2/3}$ to nonbonding, bonding Si(sp^3)-Co(3*d*), and bonding Si(sp^3)-Co(4*s*) states. Interestingly, it is noted that the nonbonding structure is more pronounced in the island region than in the flat region, suggesting a weaker Si-Co hybridization in the chemisorbed flat region.

As an example of "nano-XPS," $3d_{3/2}$ and $3d_{5/2}$ core spectra are measured in the In 3D island and In double-layer regions on a Si(111) surface, as denoted by circles in the inset of Fig. 3. To obtain the surface in which 3D islands and the double In layer coexist, we evaporated In onto the Si(111)7×7 surface at approximately 500 ºC and cooled it to room temperature during the evaporation. The spectrum obtained from the double layer is decomposed into two components, which may be considered to be as to originating from surface and interface atoms with charge transfers in opposite directions to each other.

As a new development, we are now improving the spatial resolution of PEEM by correcting the spherical aberration by the "moving focus method (MOF)" proposed by Ikuta [3,4]. This project, supported by MEXT, is now being carried out by Koshikawa's group [5]. Sub-ten-nm-resolution XPS images are expected. The PEEM images that were tentatively obtained with a Hg lamp in a laboratory at Osaka Electro-Communication University is shown in Fig. 4. This method will be applied to SR-SPELEEM in the near future in order to improve the resolution.

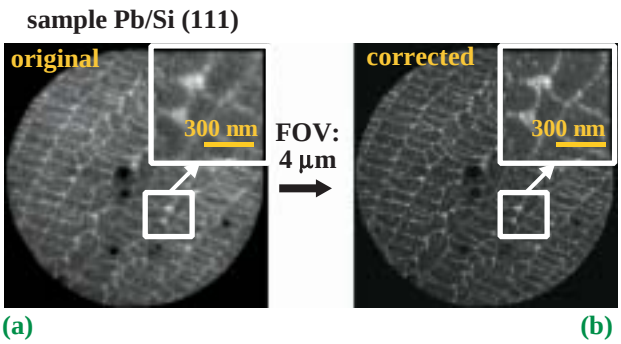

Fig. 4. **(a)** Original PEEM image, **(b)** PEEM image with aberration corrected by "MOF."

Takanori Koshikawa[a,*], Keisuke Kobayashi[b] and Fangzhun Guo[b]

(a) Fundamental Electronics Research Institute, Osaka Electro-Commun. University
(b) SPring-8 / JASRI

*E-mail: kosikawa@isc.osakac.ac.jp

References

[1] Th. Schmit et al.: Surf. Rev. Letters **5** (1998) 1287.
[2] *F.Z. Guo, T. Wakita, H. Shimizu, T. Matsushita, T. Yasue, T. Koshikawa, E. Bauer and K. Kobayashi: J. Phys.: Condens. Matter.* ***17*** *(2005) 1363.*
[3] T. Ikuta: Appl. Opt. **24** (1985) 204.
[4] T. Ikuta: J. Electron Microsc. **38** (1989) 415.
[5] *T. Koshikawa, H. Shimizu, R. Amakawa, T. Ikuta, T. Yasue and E. Bauer: J. Phys.: Condens. Matter.* ***17*** *(2005) 1371.*

Development of Monochromator Stabilization System

The stability of a photon beam is a serious problem in the case of third generation light sources. A beam position stability in the order of microns is required to transport a small beam to a sample position, at a distance of more than 50 m from the source point. In SPring-8, due to the efforts to improve the performance of the storage ring, the fluctuation of the electron beam orbit was reduced to few μm per day. However, instabilities in the photon beam intensity and in the position at the sample location were observed.

One of these instabilities is caused by the double-crystal monochromators (DCM). The DCM is equipment used to tune the X-ray energy via the Bragg reflection of the two monochromator crystals with a parallel arrangement. If there is an instability in the parallel arrangement, the energy, position, and intensity of the exit beam become unstable. Moreover, since many users set a slit width of less than 100 μm × 100 μm for a sample, the beam position fluctuation causes a further instability in beam intensity. To stabilize the exit beam from the DCM, we introduced the monochromator stabilization system (MOSTAB). This was originally designed as a system that maintains a constant beam intensity [1], and has been widely used at synchrotron radiation facilities.

We developed a MOSTAB with mode selectivity for stabilizing the beam position or intensity in SPring-8 [2,3]. Since the beam position and intensity from the DCM correlate with each other, both are similarly stabilized by single feedback control. The MOSTAB is shown in Fig. 1. The beam position or intensity is measured using a beam position monitor (BPM) [4] or an ionization chamber, and is fed to a control electronics system with an embedded a digital signal processor. It calculates the feedback voltage that is applied to a high-voltage amplifier for driving a piezo translator (PZT). Then the angle of the first crystal of the DCM is tuned by the PZT. A workstation-based control software automatically provides proper feedback parameters to the system at any energy setting of the DCM [5]. The software also enables or disables the MOSTAB on the basis of the status of the beamline and storage ring. All the hard X-ray beamlines in SPring-8 have identical SPring-8 standard monochromator and control systems; hence, it is easy to install the MOSTAB. Presently, 13 beamlines utilize the MOSTAB. Figure 2 shows the result of beam position stabilization with the MOSTAB at R&D beamline BL46XU.

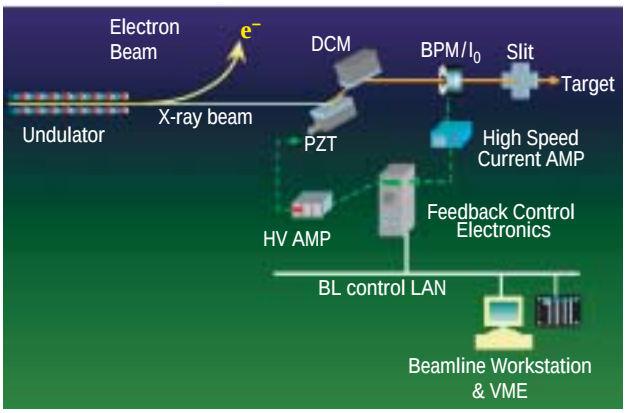

Fig. 1. Schematic diagram of MOSTAB. In this diagram, the feedback electronics is controlled by a workstation-based software. In addition, we have developed a PC-based control software as an alternative.

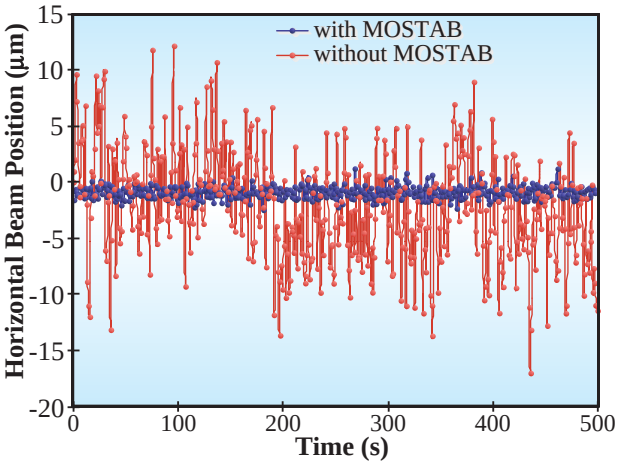

Fig. 2. Beam position stabilization using MOSTAB and BPM at beamline BL46XU experimental hutch. The standard deviation of the beam position was reduced from 4.9 μm to 0.5 μm. The beam energy provided by the Si(111) DCM was 24 keV.

Togo Kudo

SPring-8 / JASRI

E-mail: kudo@spring8.or.jp

References

[1] A. Krolzig *et al.*: Nucl. Instrum. Meth. **219** (1984) 430.
[2] Y. Nishino *et al.*: Proc. of SPIE **5195** (2003) 94.
[3] *T. Kudo, Y. Nishino, M. Suzuki, H. Tanida, Y. Furukawa, T. Hirono and T. Ishikawa: J. Jpn. Soc. Synchrotron. Rad. Res.* ***16*** *(2003) 173.*
[4] R. Alkire *et al.*: J. Synchrotron Rad. **7** (2000) 61.
[5] Y. Furukawa: BioXHIT Workshop on Automated X-ray Provision, ESRF, Grenoble, France (2004).